Your comments will be most welcome.

# TRANSITION AND TURBULENCE IN FLUID FLOWS AND LOW-DIMENSIONAL CHAOS

K.R. Sreenivasan
Yale University

Text of the talk presented on June 11, 1984 at a meeting in Northwestern honoring Professor S. Corrsin, to appear in the Springer-Verlag book 'Fundamentals of fluid mechanics' (S.H. Davis, J.L. Lumley, eds.).

# TRANSITION AND TURBULENCE IN FLUID FLOWS AND LOW-DIMENSIONAL CHAOS

K.R. Sreenivasan
Yale University

ABSTRACT

Recent studies of the dynamics of low-dimensional nonlinear systems with chaotic solutions have produced very interesting and profound results with several implications in many disciplines dealing with nonlinear equations. However, the interest of fluid dynamicists in these studies stems primarily from the expectation that they will help us understand better the onset as well as dynamics of turbulence in fluid flows. At this time, much of this expectation remains untested, especially in 'open' or unconfined fluid flows. This work is aimed at filling some of this gap.

Measurements made in the wake of a circular cylinder, chiefly in the Reynolds number range of about 30-$10^4$, have been analyzed to show aspects of similarity with low-dimensional chaotic dynamical systems. In particular, it is shown that the initial stages of transition to turbulence are characterized by narrow windows of chaos interspersed between regions of order. The route to the first appearance of chaos is much like that envisaged by Ruelle & Takens; with further increase in Reynolds number, chaos disappears and a return to three-frequency quasiperiodicity occurs. This is followed in turn by the reappearance of chaos, a return to four-frequency quasiperiodicity, reappearance of chaos yet again, and so on. We have observed several alternations between order and chaos below a Reynolds number of about 200, and suspect that many more exist even in the higher Reynolds number region. Each window of chaos is associated with a near-discontinuity in the vortex shedding frequency and the rotation number, as well as a dip in the amplitude of the vortex shedding mode. It is further shown that the dimension of the attractor constructed using time delays from the measured velocity signals is truly representative of the number of degrees of freedom in the ordered states interspersed between windows of chaos; it is fractional within the windows of chaos, and is higher than those in the neighbouring regions of order. Our measurements suggest that the dimension is no more than about 20 even at a moderately high Reynolds number of $10^4$, and that it probably settles down at about that value.

CONTENTS

## 1. INTRODUCTION

### a. General remarks

The principal parameter of incompressible viscous flows, in situations free of body forces, is the Reynolds number, Re. Observations show that for given (fixed or time-independent) boundary conditions (and external forces if applicable), the flow is unique and steady for $Re < Re_{cr}$, where $Re_{cr}$ is a certain critical value of Re; this is the steady laminar motion. As Re increases, the fluid motion may first become periodic, quasiperiodic, and 'eventually' chaotic. (Chaos is defined better in section 3 and in the appendix, but we shall also loosely use the word to designate a state in which the details of motion are not reproducible.) This chaotic state is not necessarily turbulence as generally understood — and we shall discuss this shortly — but it is believed that one attains the turbulent state if the Reynolds number is taken to a sufficiently high value. The goal of the stability theory is to understand how the evolution from the laminar to the turbulent state occurs, while turbulence theories aim at unearthing and predicting the mysteries of the (fully) turbulent state itself.

It is generally believed that the key to both these problems lies in the Navier-Stokes (NS) equations, and that no additional hypotheses of fundamental nature are required for describing either the onset of turbulence or its dynamics. Much effort has thus been spent on mastering the NS equations. However, the difficulties, both analytical and computational (at high enough Reynolds numbers), remain intimidating.

In the recent past, claims have been made that autonomous dynamical systems with small number of degrees of freedom, typified by

$$\frac{db_i}{dt} = f(b_i;\ \varepsilon_i), \tag{1.1}$$

where the $b_i$ characterize the state of the system (the so-called 'state variables'), i is a small integer, and $\varepsilon_i$ are the so-called control parameters (analogous to Re in the NS equations), help us towards attaining both the goals mentioned above. It is to a discussion of aspects of these claims, via an example of fluid flow behind circular cylinders, that this paper is devoted.

b. Remarks on degrees of freedom, genericity, and spatial chaos

Several questions arise immediately. One natural question concerns the relevance to fluid flows of low-dimensional dynamical systems. To give some meaning to the concept of degrees of freedom in fluid flows, let us *approximate* the velocity vector $u_j$ appearing in the NS equations as

$$u_j = \sum_{\underset{\sim}{k}} a_j(\underset{\sim}{k};t)e^{i\underset{\sim}{k}\cdot\underset{\sim}{x}} \quad (j = 1,2,3), \tag{1.2}$$

where the wave number vector $\underset{\sim}{k}$ is an element of a discrete (finite or infinite) set. The NS equations can then be written formally as

$$\frac{\partial a_i(\underset{\sim}{k};t)}{\partial t} = F(a_i;\ \mathrm{Re}),\ i = 1,2,....N\ (\text{large}). \tag{1.3}$$

The number of the coefficients $a_i$ which, for given boundary conditions for the fluid flow, are capable of variation in time can now be called the degrees of freedom of the fluid flow governed by the NS equations (to within the approximation implied in (1.2) and (1.3)). Since the laminar flow is uniquely specified by the boundary (and external force) conditions, this number is zero. If Re increases just past $\mathrm{Re}_{cr}$, only a few degrees of freedom are excited, and hence it appears that, at least in the positive neighbourhood of $\mathrm{Re}_{cr}$ (to be called transcritical region henceforth), consideration of these few degrees of freedom is adequate.

An interesting hypothesis (which we shall examine in this paper) is that the number of degrees of freedom (not necessarily in the sense described above) remains small even in (certain type of) high Reynolds number turbulence.

Assuming that the number of degrees of freedom excited in the transcritical region is indeed small, we must ask whether the behavior in this transcritical region does not depend on the broad nature of the right hand side of equations (1.1) and (1.3). The most often cited justification for the belief that this dependence is in some sense of secondary importance comes from the work of Ruelle & Takens [1] and Newhouse, Ruelle & Takens [2] which indicates that chaos sets in abruptly following a few Hopf bifurcations, and that this behavior is 'generic' or 'typical'.

The words 'generic' and 'genericity' find their frequent use in the literature on dynamical systems, and so, it is perhaps useful to discuss the concept briefly. Ruelle & Takens make this concept quite specific for the vector fields they were considering, but we shall be content with a rather loose qualitative description. Consider as an *example*, a class of functions possessing continuous derivatives up to a certain order, and satisfying differential equations of the type (1.1). Properties of this class of functions which are the rule and not the exception, and which do not depend on the precise nature of the right hand side of (1.1), are called generic. The conclusions of Ruelle & Takens strictly hold for an idealized mathematical system, and whether the concept of genericity is powerful enough to embrace fluid systems is not clear. One should attempt to answer this question by looking at the specific form of F in (1.3) and/or by observing the actual bifurcations in experiments on laminar-turbulent transition.

Even if the concept of genericity does hold for fluid flows, it is not obvious that interesting nongeneric phenomena do not occur. To make this notion specific, let us consider the following rather far-fetched example. Suppose we link (as in our example above) genericity to the existence of velocity fields possessing continuous derivatives of a certain order. Those generic properties may be irrelevant to a turbulent boundary layer since one cannot exclude the possibility that at some moment during bursting near the wall (a key event sustaining turbulence production) this smoothness condition is destroyed in spite of viscosity. It is therefore sensible to keep in mind that nongeneric behavior is neither uninteresting nor unlikely, especially when conditions such as configurational symmetry, vicinity to wall, play an important role in the evolution of the flow.

Finally, one must mention the predominant role played by spatial chaos (and order!) in turbulent flows of fluids. An important characteristic of fluid turbulence is random vorticity, whose presence necessarily implies that the velocity vector is a random function of *position*. Autonomous dynamical systems of the type (1.1), on the other hand, do not contain any space information. While temporal chaos in fluid turbulence may in some sense be symptomatic of spatial chaos, it is clear that autonomous dynamical systems have little to say directly about the latter, at least at the current state of development.

### c. 'Closed' and 'open' flow systems

Notwithstanding these remarks, it is necessary to note that several beautiful experiments now exist in the Taylor-Couette flow (e.g., Refs. 3, 4 and 5) and the convection box (e.g., Refs. 5 and 7) which have lent support to the notion that the behavior of fluid flows in the transcritical region could be similar to that of low-dimensional dynamical systems. This in itself is undoubtedly remarkable, but it should be remembered that these two flows are special in the following sense. In all 'closed flow' systems — of which the convection box and the Taylor-Couette flow are two popular examples — the boundary is fixed so that only certain class of eigenfunctions can be selected by the system; this does not hold for another class of flows we may call 'open flow systems' — for example, boundary layers, wakes, jets — in which the flow boundaries are continuously changing with position. Thus, while in closed flow systems each value of the control parameter (for example, the rotation speed of the inner cylinder in the Taylor-Couette problem) characterizes a given state of the flow globally, this is not true of open systems. Consider as an example the near field of a circular jet. For a given set of experimental conditions, the flow can be laminar at one location, transitional at another and turbulent at yet another (downstream) location. This usually sets up a strong coupling between different phenomena in different spatial positions in a way that is peculiar to the particular flow in question. Secondly, the nature and influence of external disturbances (or the 'noise', or the 'background or freestream turbulence') is more delicate and difficult to ascertain in open flows: the noise, which is partly a remnant of complex flow manipulation devices and partly of the 'long range' pressure perturbations, is not 'structureless' or 'white', no matter how well controlled. Finally, it is well known that closed flow systems can be driven to different states by means of different start-up processes; for example, different number of Taylor vortices can be observed in a Taylor-Couette apparatus depending on different start-up accelerations [8]. This type of path-sensitivity in a temporal sense does not apply to open systems, where the overriding factor is the path-sensitivity in a spatial sense (i.e., the 'upstream influence').

### d. Scope of the paper

On balance, all these considerations suggested to us that it is desirable to look at some open flows to determine the extent to which dynamical systems can assist us in our goals of understanding transition and turbulence in fluid flows. This is the motivation for the work described in this paper, which is to be viewed more as a progress report than as a complete account; obviously much more remains to be done. Our approach is to select well-known flows and follow the bifurcations as closely as possible. (We reported some of our earlier work in pipe flows in [9] and wake work in [10].) Surprisingly, while much work has been done in these flows in the past, an

amazing amount of new information can still be acquired that will facilitate clarifying the relation between low-dimensional chaotic systems and fluid flow transition and turbulence. Part of the reason for this is undoubtedly that the details one looks for are often dictated by contemporary concerns.

## 2. EXPERIMENTS

### a. Experimental conditions

Although we have conducted experiments in wakes, jets and pipe flows, we choose to discuss here only our wind tunnel experiments in two-dimensional wakes behind circular cylinders. The Reynolds number range covered is from about 30 (slightly below the vortex shedding value) to about $10^4$. Two wind tunnels — one of the blower type and one of the suction type — were used. Nylon threads, stainless steel wires and aluminium tubes, stretched tightly across the width of the wind tunnels, were used as wake generators. The aspect ratio varied between about 70 and 2000. The basic experimental conditions are summarized in Table 1.

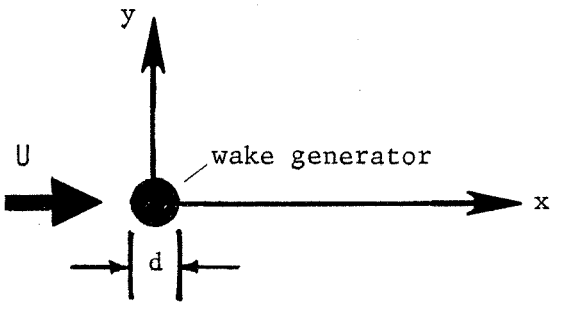


| d (mm) | ≈x/d | ≈y/d | aspect ratio | wind tunnel characteristics |
|---|---|---|---|---|
| 0.24 | 5 | 1 | 2000 | suction type; turbulence level ≈ 0.2% at speeds of interest |
| 0.24 | 50 | 1 | 2000 | |
| 0.36 | 5 | 1 | 1330 | |
| 4.0 | 5 | 1 | 170 | |
| 0.36 | 11 | 1 | 70 | blower type; turbulence level varied from 0.68% at speeds ≈ 1 m/s to 0.06% at speeds ≈ 10 m/s |

Table 1. The flow configuration and experimental conditions

All velocity signals were obtained with a hot-wire operated on a DISA 55M01 constant temperature anemometer. The speed of the tunnel was monitored with a Pitot tube connected to a calibrated MKS Baratron with adequate resolution ( and an aver-

ager). The hot-wire and the Pitot tube were mounted on a specially designed slim holder.

Some of the data to be presented in this and later sections is in the form of power spectral density of the streamwise velocity component, u. Nearly all the signals were digitized at sufficiently high frequency (60 kHz or more) to ensure that, whenever the signal was periodic, at least 30 digitized points were contained in one period of the basic frequency (so that it was a good representation of the analog signal). Further, the entire length of the signal (which contained at least 100 cycles of the basic frequency) was Fourier transformed at once using the Cooley-Tukey FFT algorithm. The overriding criterion was that the spectral resolution should be as good as possible (here, between 0.5 Hz and 2 Hz compared with shedding frequencies of the order of 2000 Hz or more) and that one must not miss any low frequency modulations.

### b. The background turbulence

We have worked with varying levels of background turbulence, and found that the occurrence of different stages of transition reported here is in itself not terribly sensitive to the turbulence level as long as it is not too high; larger turbulence levels blur the distinction between different stages and alter the details somewhat erratically. One should, however, strive to eliminate all strong discrete frequency components in the background turbulence structure.

Figure 1a shows a typical power spectral density of u in the freestream at Re = 60. (The ordinate is the logarithm to base 10 of the power.) The 'noise' (though devoid of any discrete peaks) does not appear to be 'white' but has a much larger low frequency component. Figure 1b shows the power spectral density measured with the flow completely shut off, but the hot-wire and other electronic instruments operating the same way as before. It is clear that the anomalously high low frequency content is not representative of the flow itself, but of electronic and computer noise. Allowance should thus be made for this fact in the interpretation of the spectral data to follow.

## 3. RESULTS FROM SPECTRAL MEASUREMENTS

### a. Route to chaos: the first appearance

Figure 2 shows the logarithm (to base 10) of the normalized power spectral density of u at a Reynolds number (based on the freestream velocity and the diameter of the cylinder) of about 36, which is approximately the onset value for vortex shedding. Notice that the instrumentation and other noise level is around $10^{-8}$, while

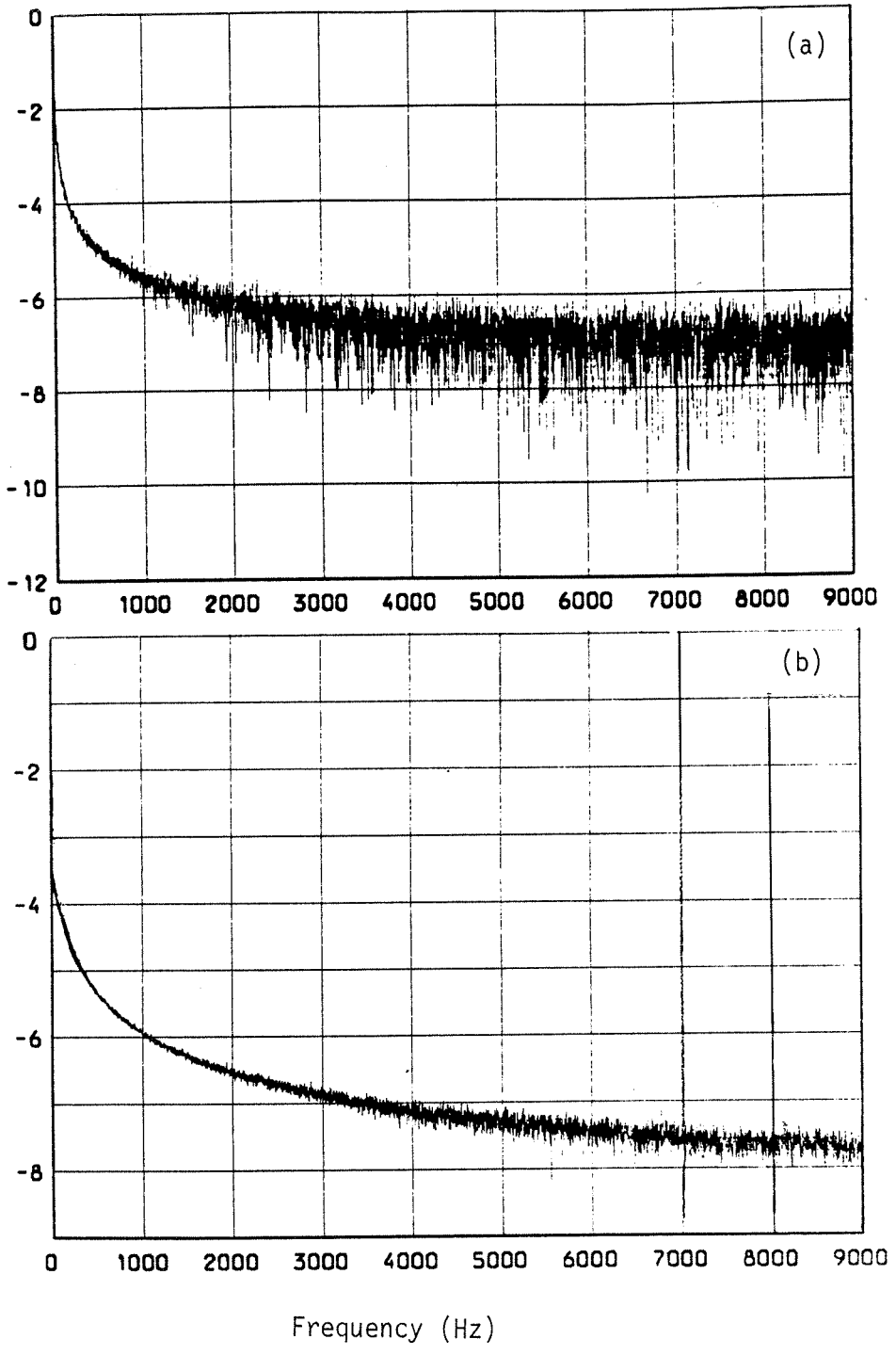


FIGURE 1: Normalized power (or frequency) spectrum of (a) noise of the instrumentation and digitizer, plus freestream disturbances, Re = 60; (b) instrumentation and digitizer noise only with no flow.

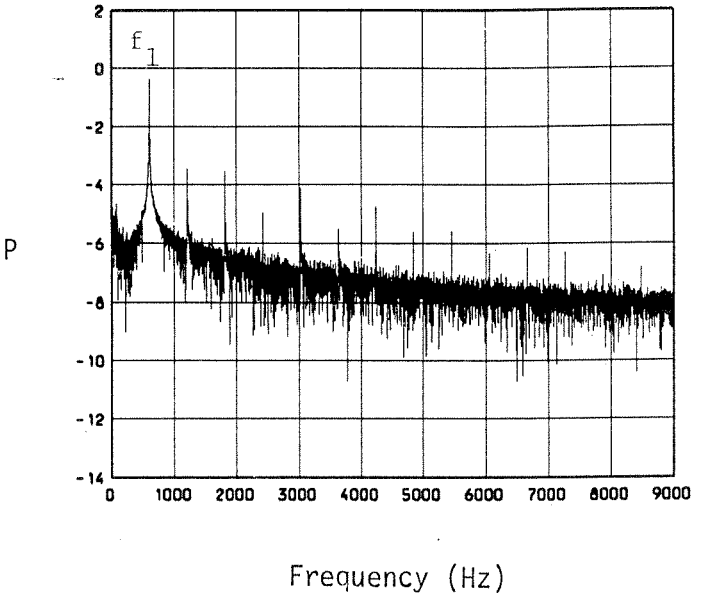


FIGURE 2: Normalized frequency spectrum of u at Re $\approx$ 36. Note that the power P is plotted on a logarithmic scale (to base 10). The peak at $f_1 \approx$ 590 Hz corresponds to the vortex shedding, and the subsequent strong peaks above the noise level are simply harmonics of $f_1$.

the peak of the spectrum (marked $f_1$), corresponding to the basic vortex shedding frequency behind the cylinder, is at round $10^{-0.5}$, about 7½ orders of magnitude higher than the noise level! The sharpness of the peak (as well as of the other peaks to the right of $f_1$ which are the harmonics of $f_1$) is excellent.

At a somewhat higher Reynolds number of 54, there appear a number of peaks in the spectrum (figure 3a); as shown in the expanded version (figure 3b) all the peaks can be identified precisely in terms of the interaction of the two frequencies — the basic vortex shedding frequency $f_1$ and another incommensurate frequency $f_2$.

At an Re = 66 the spectrum (figure 4) shows broadened peaks with no overwhelmingly strong discrete components — quite a different situation from that of figures 2 and 3. One might say, in the language of dynamical systems, that chaos has set in!

The sequence of events leading to chaos are so far literally like that envisaged in the Ruelle-Takens-Newhouse (RTN) picture of transition to chaos, and so, a brief digression *roughly* describing this picture is quite useful. (The appendix is an introduction to the basic terminology.) With increasing Re, the steady laminar motion loses stability and becomes periodic with frequency $f_1$ (say); the power spectral density will have (as in figure 2) a peak at $f_1$ (and its harmonics), and the phase diagram will show a limit cycle behavior. Loss of stablility of this new state yields a quasiperiodic motion with two independent frequencies, $f_1$ and (say) $f_2$. The spectral density will now show $f_1$, $f_2$ and various combinations $mf_1 \pm nf_2$ (as in figures 3a, b), and the phase portrait will be a two-torus. Further increase in Reynolds number yields a quasiperiodic motion with three frequencies (three-torus ). New-

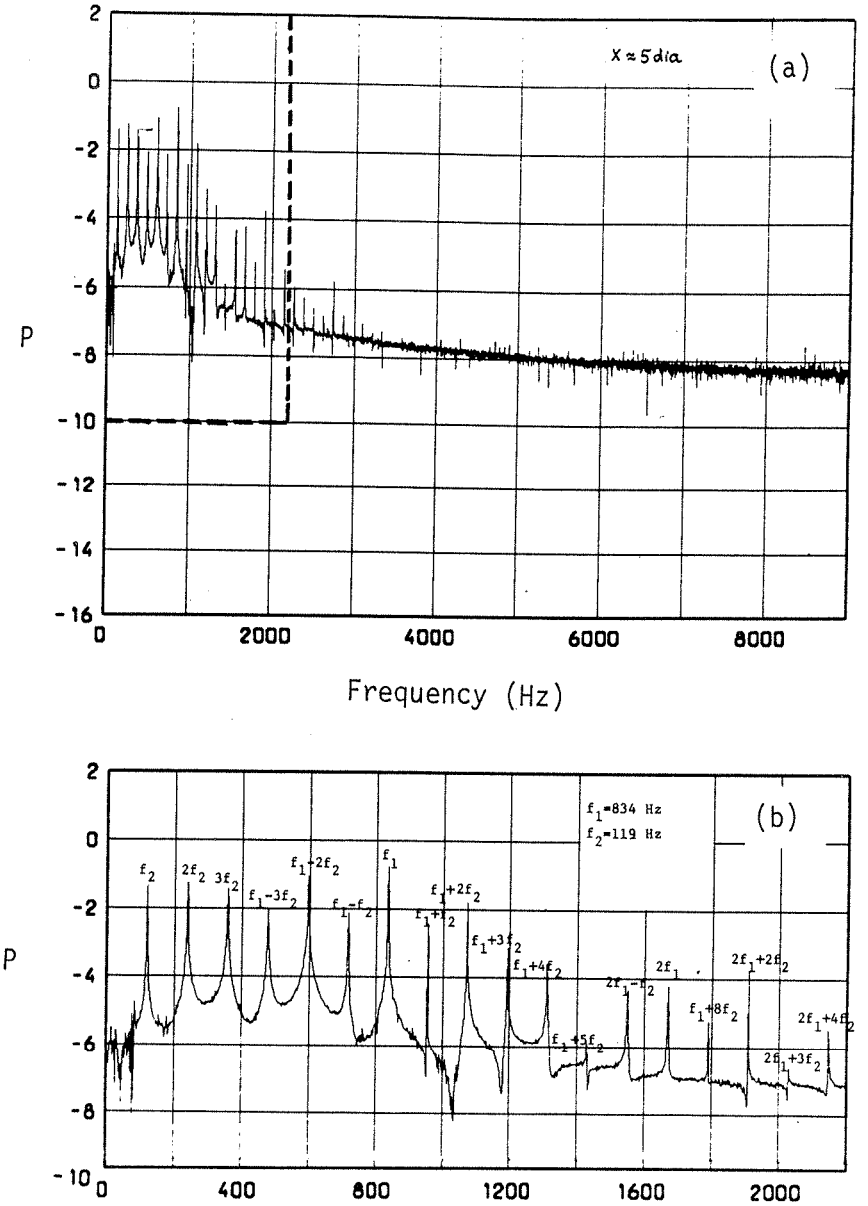


FIGURE 3: (a) Normalized frequency spectrum of u at Re = 54. In (b), the frequency range 0-2200 Hz is expanded. All significant peaks in (b) are simple combinations of the vortex shedding frequency $f_1$ (corresponding to the most dominating peak), and another incommensurate frequency $f_2$. After satisfying ourselves that there are no subharmonics of $f_1$ (and that 119.02 Hz is unrelated to the line frequency or spurious oscillations of the cylinder) we have picked $f_2$ by hypothesizing that the peaks nearest $f_1$ must be $f_1 \pm f_2$. The value of $f_2$ thus obtained accounts for every other significant peak as shown in (b) — actually to 4 or 5 decimal places for reasons we do not understand! At least part of the reason for the relatively low noise level (compared with figure 2) is the increased signal level.

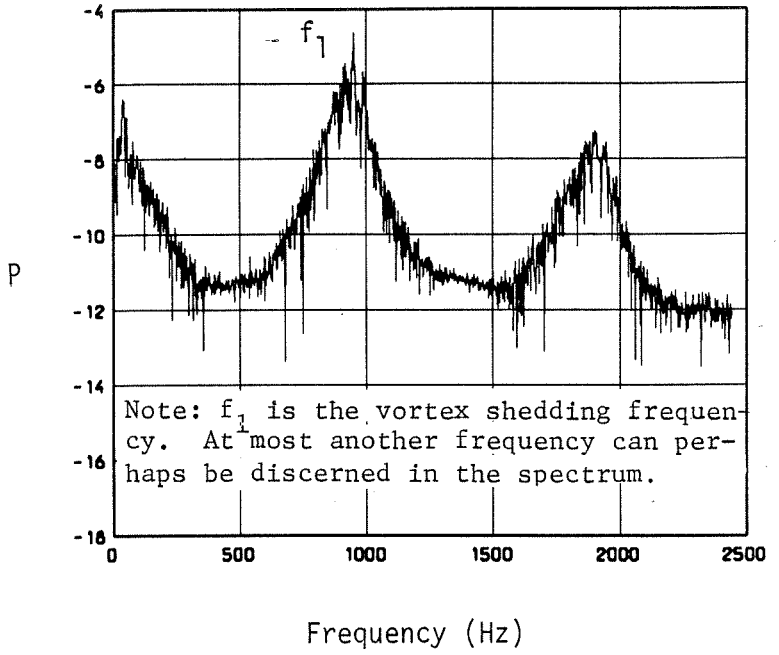


FIGURE 4: The first appearance of chaos at Re = 66. The broadband nature implies chaos; onset of chaos does not rule out the existence of spectral peaks. (Note: This does not signify some high order quasiperiodicity as dimension and entropy calculations of section 4 show.)

house, Reulle & Takens [2] argue that even a weak nonlinear coupling (of a certain variety!) among the three frequencies is likely to result in chaos or a strange attractor (see appendix), one of whose symptoms is an increased broadband content (see figure 4). This contrasts the classical picture of Landau, according to which turbulence is the asymptotic state of increasingly higher order quasiperiodicities.

Phase diagrams provide complementary information on the sequence of events leading to chaos. To construct phase diagrams, it would seem that one would require the measurement of N independent variables (in general, a hopeless task!), but embedding theorems like those of Takens [11] justify the use of a single measured variable. From the measured local velocity u(t) — for example — one constructs a d-dimensional diagram from the vectors $\{u(t_i), u(t_i + \tau), \ldots. u(t_i + (d-1)\tau)\}$, $i = 1, \ldots\infty$, $\tau$ being a time delay whose precise value in a certain wide range seems to be immaterial. According to the embedding theorems, the phase diagrams constructed in the above manner will have essentially the same properties as the one with N independent variables, as long as $d \geq 2N + 1$ (although exceptions to this now commonly assumed philosophy are not hard to concoct). In practice, d is increased by one at a time until the properties of interest become independent of d.*

* About two years ago (October 1982) when we first started constructing phase diagrams in this manner, we were unaware of any literature on embedding theorems, but were guided solely by elementary *ad-hoc* considerations.

Figures 5, 6 and 7 show respectively the plot of $u(t_i + \tau)$ vs $u(t_i)$ at Re = 36, 54 and 66, and can be considered as projections of the phase diagrams on a two-dimensional plane. The limit cycle behavior at Re = 36 is evident, the scatter visible in the figure being partly due to experimental noise (see figure 2) and partly due to the jitter in the signal. Further, a Poincaré section reveals no discernible structure. The situation is thus basically periodic.

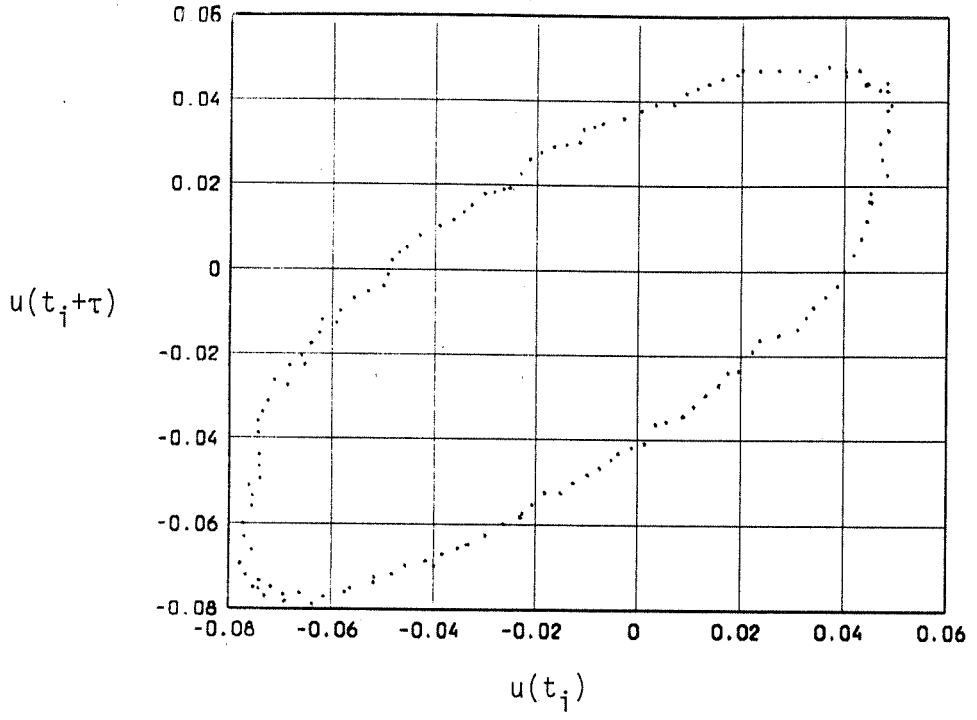


FIGURE 5: The phase plot from the velocity signal u at Re $\approx$ 36, showing limit cycle behavior. The time delay $\tau$ = 10 sampling intervals; the starting point $t_1$ is arbitrary.

At Re = 54, although the projection of the phase diagram is complicated in appearance*(figure 6a), a Poincaré section (figure 6b) yields a limit cycle, reinforcing the fact that only two degrees of freedom are present. On the other hand, not only is the projection of the phase diagram at Re = 66 complex (figure 7), but also its Poincaré sections (not shown), no matter how defined. This, as well as the fractional dimension of the attractor (see section 4a) show that the signal is indeed chaotic.

(As equally valuable measures of chaos, one could evaluate the Lyapunov exponent (characterising the exponential divergence of nearby trajectories) or the Kolmogorov entropy (which, for typical systems, equals the sum of positive Lyapunov exponents). Limitations of various kinds have prevented us from measuring the Lyapunov exponent — such measurements for a Taylor-Couette flow have been made by Brandstäter et al. [5] — but we do discuss some entropy measurements in section 4d.)

---

* Note that the trajectory resides most often in the upper right quadrant, but only rarely strays away into the lower left quadrant. This behavior in the phase plane can be related to the finite skewness of the signal.

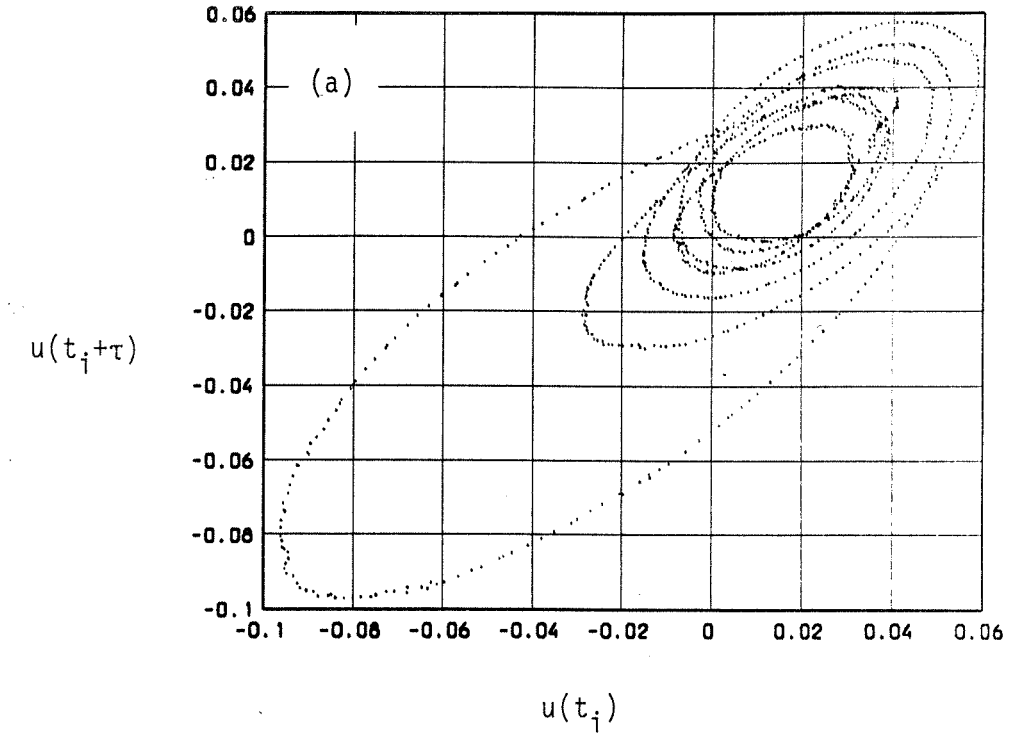


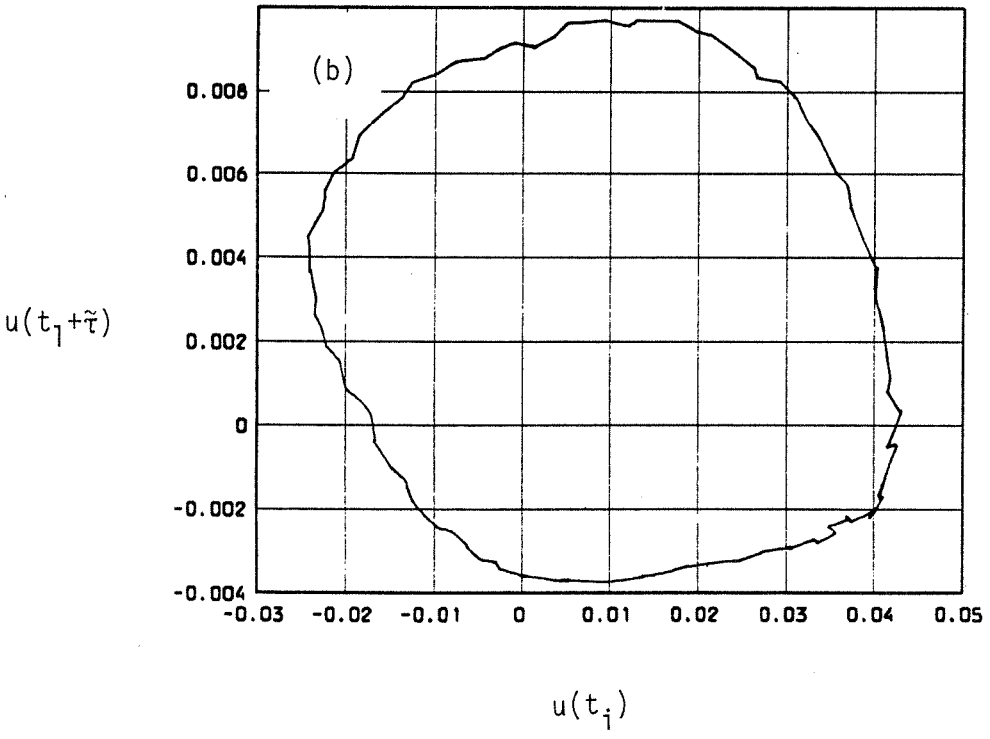


FIGURE 6: (a) The phase plot from u at Re $\approx$ 54. $\tau$ = 10 sampling intervals. (b) Poincaré section for the phase plot of (a). This is simply a plot of $u(t_i+\tilde{\tau})$ vs $u(t_i)$ with $\tilde{\tau}$ spaced exactly $1/f_2$ apart.

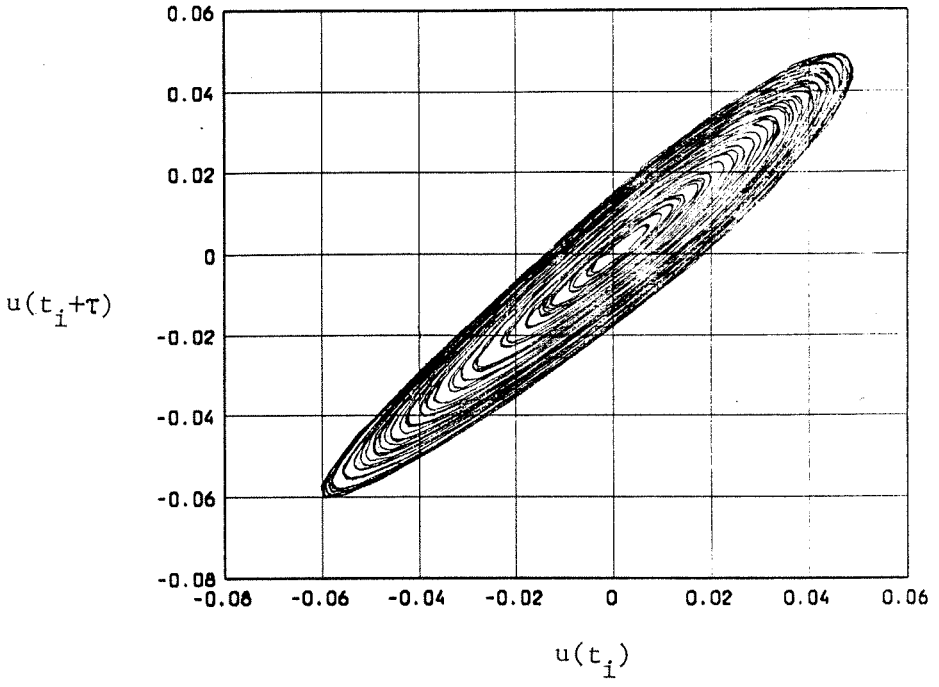


FIGURE 7: The phase diagram for Re = 66. $\tau$ = 10 sampling intervals. The continuous curve is now the result of joining successive data points (done for clarity).

This progression towards chaos — underlying the possible presence of a strange attractor — proceeds much like that proposed by Newhouse, Ruelle & Takens [2]. It is thus extraordinary that the 'generic' behavior indicated by Ruelle & Takens for an idealized mathematical system should have a nontrivial bearing on a rather complex fluid dynamical system!

It should be noted that few would feel comfortable in designating as turbulent the *signal* we have recognized as chaotic. Clearly, to the extent that a turbulent *flow* must possess *spatial* randomness, we cannot say much of value as to whether the *flow* at Re = 66 is turbulent or not without a global survey of the flow field at this Reynolds number. Further, if one *defines* turbulence as a high Reynolds number phenomenon (as is often done!), it is tautologically true that the signal does not represent turbulence. Further, a look at the signal (figure 8) would prevent someone

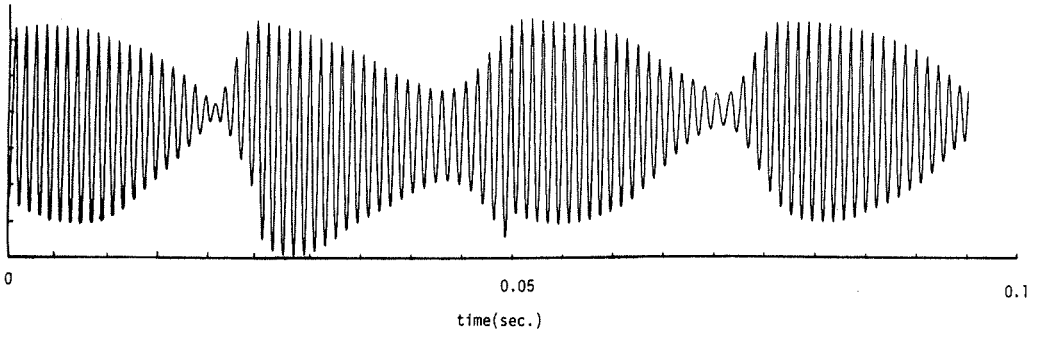


FIGURE 8: The signal u(t) at Re = 66.

with an everyday familiarity with high Reynolds number turbulence from accepting it as turbulent. Nevertheless, we would like to suggest that the signal shown in figure 8 is indeed random (for example, in terms of algorithmic complexity required to specify it [12]) with a well-defined probability density (see figure 9; for a comparison with similar data at 'large' Reynolds numbers in the far wake, see Thomas [13]).

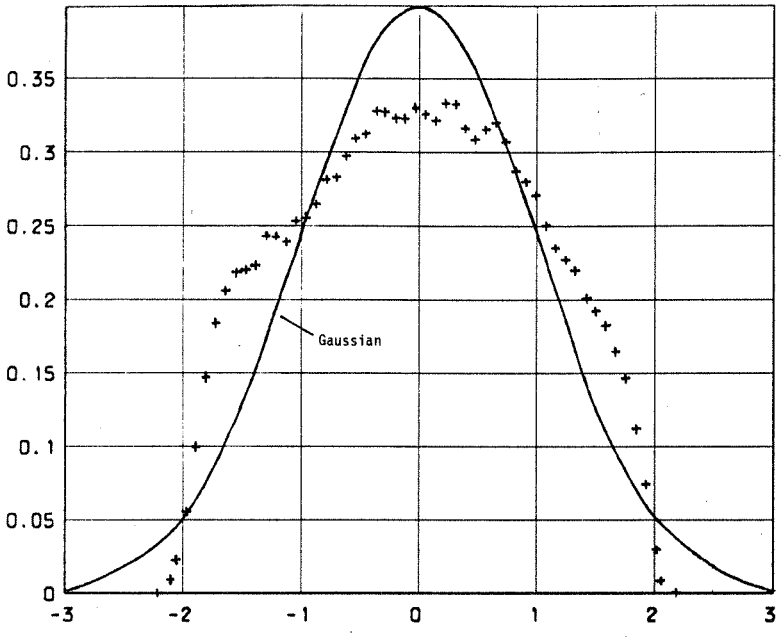


FIGURE 9: The measured probability density of u at Re = 66. The abscissa is the amplitude about the mean normalized by the root-mean-square of the signal, and the ordinate is the probability density. The signal has a skewness of near zero and a flatness of about 2.4.

What this means is that even at low enough Reynolds numbers, the interaction of only a few degrees of freedom leads to randomness! It is also pertinent to point out that at least in some respects the signal of figure 8 resembles a narrow band pass filtered turbulent signal at high Reynolds numbers. (Perhaps the word 'preturbulence' also used commonly in dynamical systems literature, is sufficiently useful to designate the signal such as the one shown in figure 8, and its dynamics.)

### b. Chaos and its aftermaths

No qualitative change occurs between Re = 66 and about 71. Soon thereafter the system becomes reordered. For example, the spectral density at Re = 76 shows (essentially) nothing but discrete peaks again (figure 10a). These peaks, shown in detail in figure 10b, can all be identified with great precision as arising from the interaction of *three* irrational frequencies. (That there are definitely three independent frequencies can also be seen from Poincaré sections (not shown here) and the dimension of the attractor discussed in section 4b). After a small increase in Reynolds

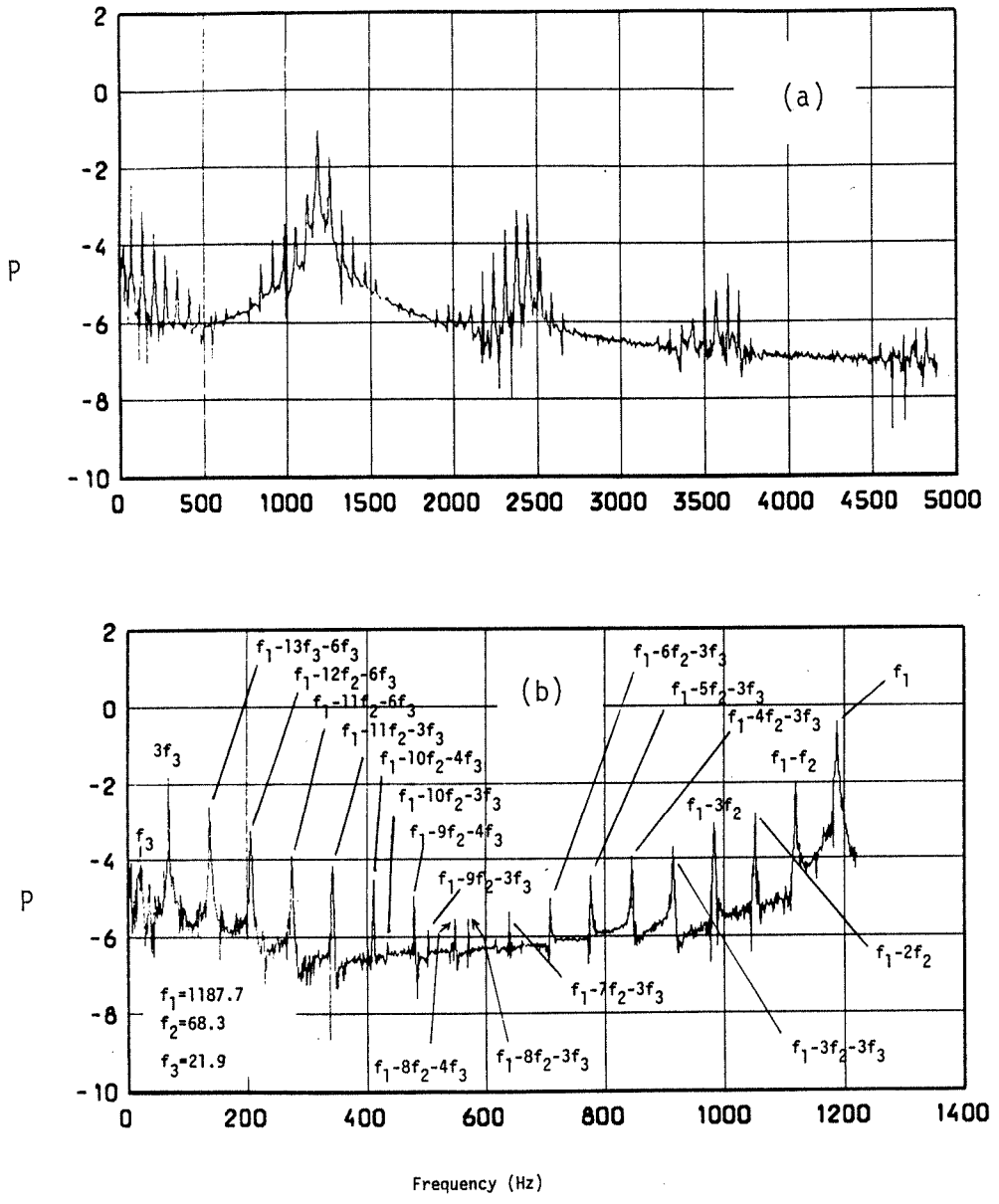


FIGURE 10: Reordering at Re = 76. (a) The measured power spectral density of u, and (b) its details in the frequency range 0-1250 Hz. Note that all peaks above noise level can be represented by combinations of three frequencies $f_1$, $f_2$ and $f_3$. This conclusion can certainly be influenced by the finite FFT resolution, but our belief in the accuracy of this statement comes also from dimension calculations (section 4).

number to about 81, one can see the onset of the broadband spectral content (figure 11), and we may consider chaos to have set in again!

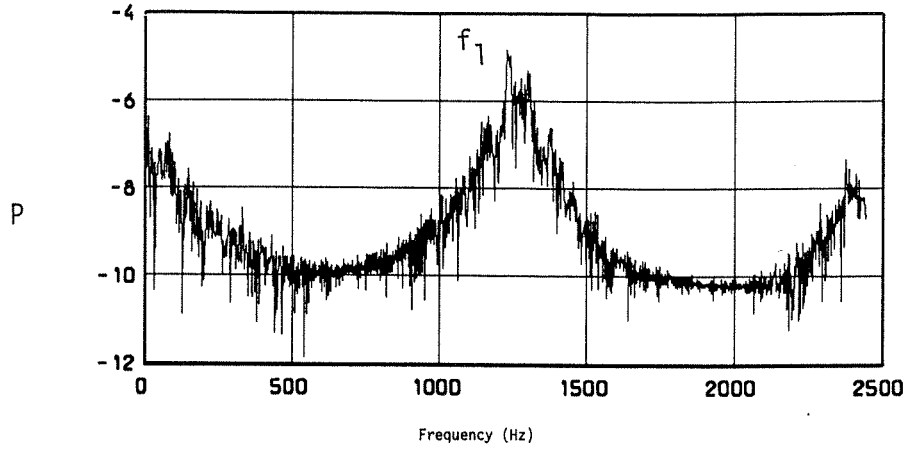


FIGURE 11: Chaos at Re = 81. $f_1$ is the vortex shedding frequency.

The system reorders itself around an Re of about 90, and we have discussed elsewhere [10] that this reordered state is quasiperiodic with four frequencies. (That this is the case will be demonstrated also by dimension measurements in section 4d.) Chaos sets in again at an Re = 140, followed by yet another reordering around an Re = 143. In fact, this sequence of return to chaos and reordering continues for much higher Reynolds numbers although it becomes progressively more difficult with increasing Re to distinguish experimentally between the two states.

Two related points of importance emerge. First, there do exist quasiperiodic motions with three or four independent frequencies; just like Landau's quasiperiodicities, the Ruelle-Takens picture of transition is also not the whole story. Second, transition to turbulence (at least in the temporal sense) is characterized by regions of chaos interspersed between regions of relative order. Each of these deserves at least a brief discussion.

### c. Note on quasiperiodicities with more than two frequencies

We have shown that the route to the lowest Reynolds number chaos occurs in our experiments precisely as postulated in the RTN picture of transition. On the other hand, our experiments also show that quasiperiodicities with three (and possibly four) frequencies do exist. This type of disagreement with the RTN scheme has been noted earlier in the Taylor-Couette flow [14] and the convection problem [15]. It is thus pertinent to inquire whether there are (in some sense) exceptional conditions to be satisfied for the RTN scheme to hold. Greborgi et al. [16], who address this question in a specific numerical experiment, suggest that the three frequency quasiperiodicity is indeed quite likely to occur in practice, and that the special perturbation required to destroy this state (as in the RTN scheme) is unlikely. Haken [17]

discusses this issue at some length and concludes that if the frequencies possess a certain kind of irrationality with respect to each other (or, more precisely, the so-called Kolmogorov - Arnold - Moser condition holds), bifurcation from a two-torus toa three-torus is possible. Both these discussions are strictly relevant to systems with no externally imposed noise (or fluctuations), a condition that does not strictly obtain in experiments (especially open systems). Our own experience is that the precise nature of even small amounts of noise (some of which is controllable in our wind tunnels and some of which is not!) has an influence on the evolution of the system (for a brief discussion of this influence, see subsection 3e). It is not hard to visualize that in our experiments the detailed conditions of intrinsic noise itself could have altered from before to after the first occurrence of chaos. Clearly, this is an area for further work, both experimentally and theoretically.

### d. Windows of order and chaos

Figure 12 summarizes the changes occurring in the low end of the Reynolds number range we have considered. The shaded regions indicate windows of chaos, and the question marks indicate the uncertainty and difficulty in quantifying what we believe are reordered states.

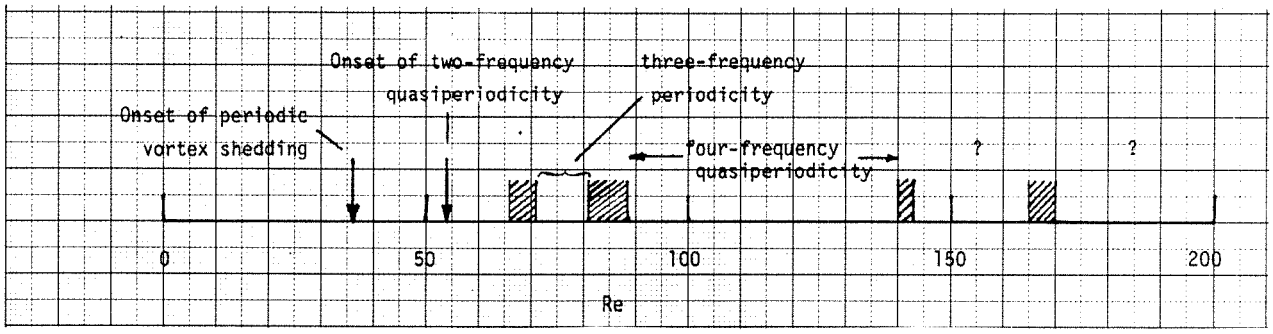


FIGURE 12: Window of chaos and order

At least two questions arise: What is the mechanism that permits the reordering of a chaotic state? What determines the length and location of the windows of chaos? Our understanding of these matters is rather limited, but even within these limits, some comments seem called for. Let us consider the first question now, and relegate the second one to the next subsection. The observed alternation between chaos and order has been known to occur in several low-dimensional dynamical systems; for example, Lorenz equations [18], and spherical pendulum [19]. In these systems, the occurrence of reordering is independent of *external* noise. The numerical experiments of Matsumoto & Ysuda [20] show that chaotic orbits could be unstable to external noise, and noise addition to deterministic chaos (i.e., chaos characteristic of deterministic dynamical systems) yields an ordered state in some cases. They specifically consider the so-called Belousov-Zhabotinskii (BZ) reaction and some variants of the logistic model. Roux et al. [21] find windows of chaos and order in their

experiments on the BZ reaction.

In experiments on open systems, it is hard to ascertain whether the return to order is tied intimately to external noise or the increased degrees of freedom associated with the appearance of chaos itself. In any case, the analogy between this situation and increased eddy viscosity in turbulent flows appears to be more than superficial: addition of high frequency modes results in a lowering of an effective Reynolds number and increased stability of the flow.

Though we have not made detailed spectral measurements at higher Reynolds numbers, it is our contention that the succession of order and chaos in a wake continues indefinitely even at very high Reynolds numbers (with the caution that order must now be interpreted to mean spectral sharpening). Roshko [22] pointed out several years ago that order reappears in the Reynolds number range of $10^6$. More recently, the fluctuating lift force measurements of Schewe [23] on a circular cylinder showed that the spectral density of the lift coefficient was broad at Re = $3.7\times10^6$ (upper end of transition) and became increasingly narrow until, at Re = $7.1\times10^6$, it was quite sharp, rather like a narrow-band-pass filtered signal. Although the fluctuating lift force can at best be related to the squared fluctuating velocity filtered via the transfer function corresponding to the response of the circular cylinder, its behavior is nevertheless indicative of the flow itself in the vicinity of the cylinder.

### e. The vortex shedding frequency and windows of chaos

Consider now the variation of the vortex shedding frequency $f_1$ with Reynolds number (figure 13). The frequency does not vary monotonically with Re but shows several more or less distinct breaks. Such breaks have been noted before [24,25,26], and perhaps most convincingly demonstrated in a beautiful experiment by Friehe [27]. Friehe varied the Reynolds number continuously at a small rate and obtained on an x-y plotter the frequency-Re variation directly. Although the appearance of the breaks has been disputed [28], our own data, presented here and elsewhere [10], support the conclusion that discontinuities do indeed appear.

Our interest here is in pointing out that the occurrence of these breaks coincides with the windows of chaos. To establish the connection better, we may consider in figure 14 the details of the break marked A in figure 13. Just upstream of the break, the spectral density is quite ordered (four-frequency quasiperiodicity) while it is broadband until the end of the break region coinciding with the upper end of the window of chaos; to the extent we can ascertain, the frequency spectrum shows a reordering immediately after the break.

The data shown by crosses in figures 13 and 14 were all obtained from one experimental run. In a repeat of the experiment the following day (for example) we found the same general features, except that chaos set in at different Reynolds numbers; the windows of chaos were also of different widths. The filled circle in fig-

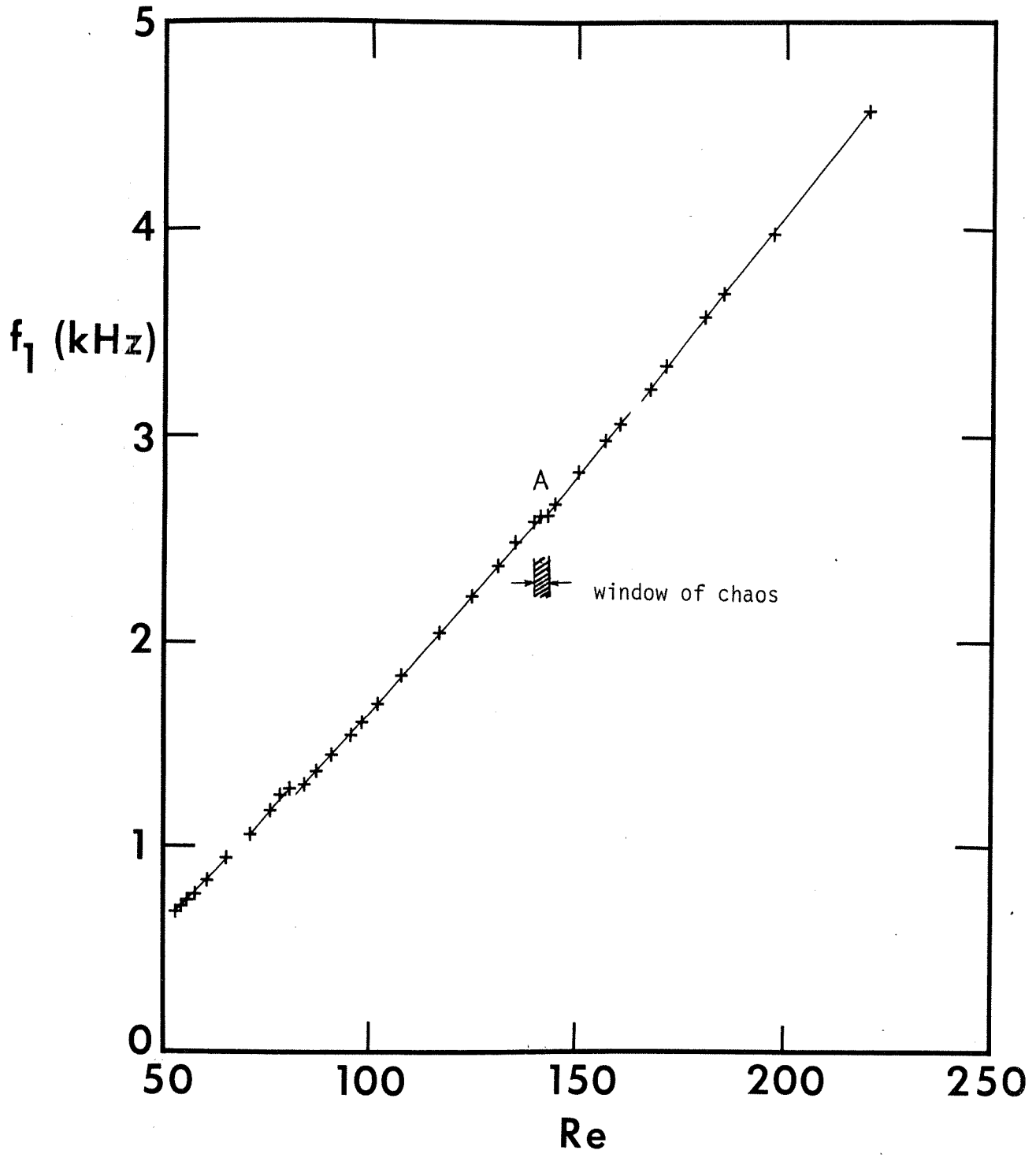


FIGURE 13: Variation of vortex shedding frequency with Re. Notice discontinuities, and their coincidence with windows of chaos, as illustrated near A.

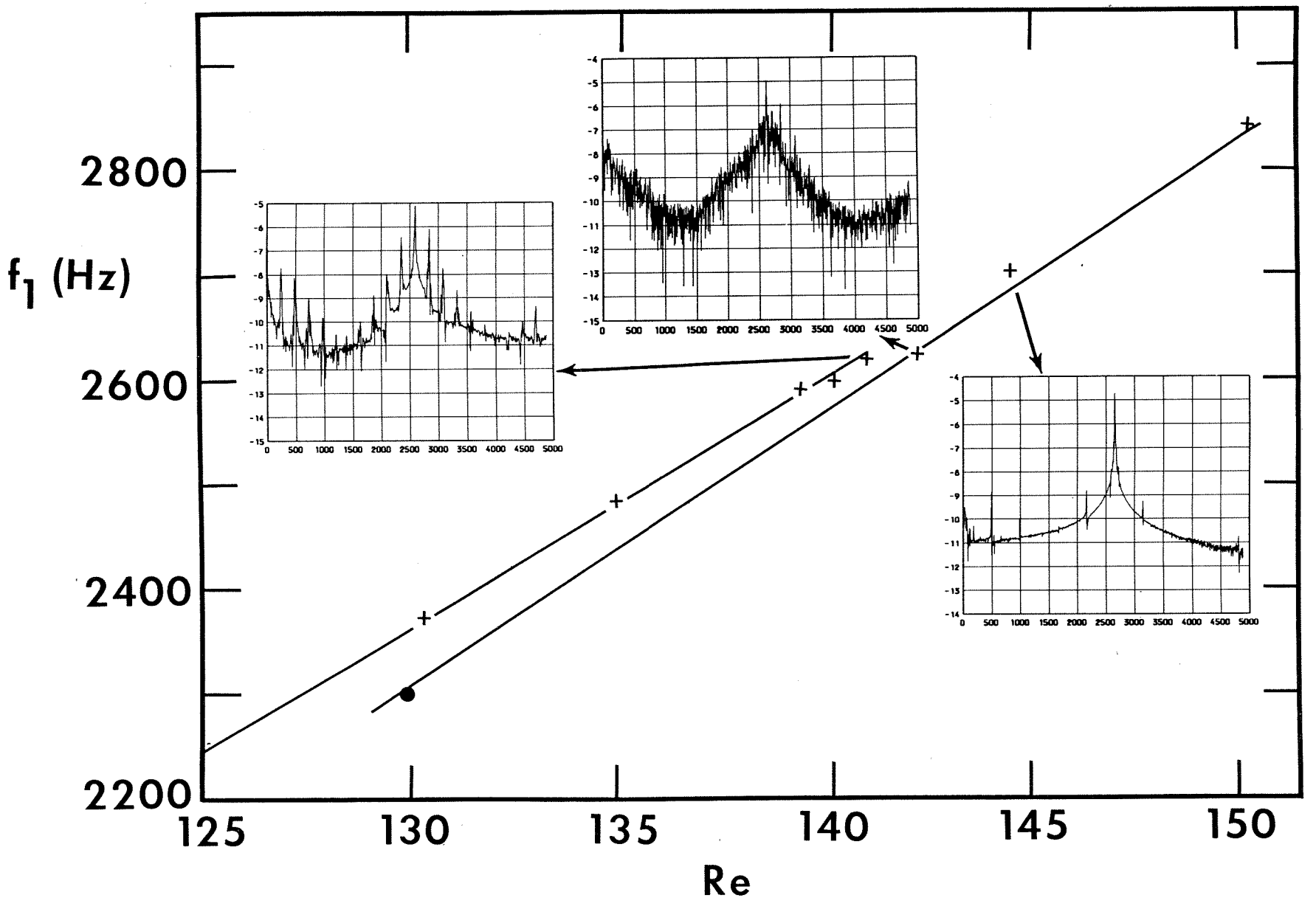


FIGURE 14: Expanded version of figure 13 near A. ● shows a data point in another series of experiments where the window of chaos began at an Re ≈ 130.

ure 14 was obtained in a second series of experiments. It is seen that this point falls below the first set of data at the same Re, but it falls on the backward extrapolation of the line corresponding to the reordered state (Re $\geq$ 143) in the first set. It is hard to tell the differences between conditions in the two experiments without extensive documentation, but there are reasons to believe that the second experiment was conducted in a somewhat noisier environment. We thus speculate that the location as well as the widths of the windows of chaos are to some extent determined by noise characteristics — in a way that is not well understood at present.

It is interesting to note from figure 14 that the ratio $f_2/f_1$ (the so-called rotation number), where $f_2$ is the second largest independent frequency, changes its value abruptly across the narrow windows of chaos. Figure 15 is a plot of the rotation number with Re. It is seen that the number changes abruptly across all the windows of chaos, but only slowly within regions of order.

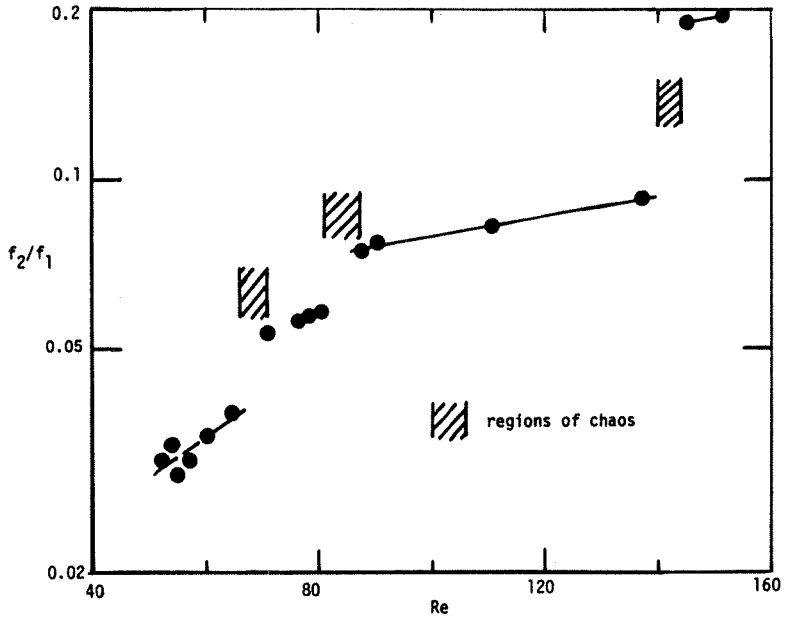


FIGURE 15: The variation of the rotation number with Reynolds number

f. The amplitude of the vortex shedding mode and chaos

Since reordering is associated with the reemergence of stronger spectral peaks, it is natural to expect that there must be some relation between the amplitudes of the various modes and the occurrence of order and chaos. Figure 16 shows the amplitude of the vortex shedding mode (or the $f_1$ frequency) as a function of velocity. (The amplitude $A_1$ is expressed as a fraction of the freestream velocity U, but is given here to an arbitrary scale.) It is clear that O indicating order coincides with a local peak in $A_1$, C indicating the onset of chaos coincides with a local minimum, and, finally, RO indicating reordering coincides with the reappearance of a peak. Except for the first time that reordering occurs, every successive reordering is associated with a

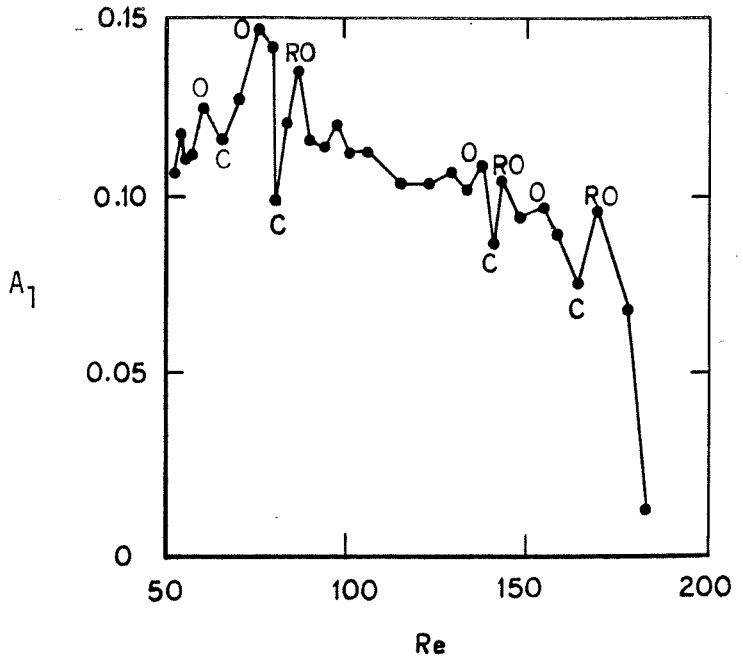


FIGURE 16: The amplitude of the vortex shedding mode as a function of Re. O is order, C chaos and RO is reordering; within a window of chaos, O and RO may in general indicate different states of order.

general lowering of the amplitude of the vortex shedding mode.

## 4. RESULTS FROM THE DIMENSION OF THE ATTRACTOR

### a. The dimension

It is clearly worth inquiring whether there is any property of the attractor that successfully describes in some way the many subtle changes that occur in the frequency spectra and the related properties discussed in section 3. It appears that there indeed is such a quantity, namely the dimension of the attractor. Loosely speaking, the dimension of the attractor is related to the number of degrees of freedom — and hence its importance. The concept of the dimension is highlighted in studies of dynamical systems, and we may briefly digress here to discuss its meaning before presenting results from our measurements. It should be pointed out that, apart from our own earlier measurements of the dimension for turbulence attractors [9,10], such measurements have been made by others in the Taylor-Couette flow [5] and in the convection cell [29].

Let us consider an attractor (constructed as already discussed in section 3) from a measured temporal signal u(t) that is embedded in a (large) d-dimensional phase space. Let $N(\varepsilon)$ be the number of d-dimensional cubes of linear dimension $\varepsilon$ required

to cover the attractor to an accuracy $\varepsilon$. Obviously, making $\varepsilon$ smaller renders N larger, but if the limiting quantity

$$D = \lim_{\varepsilon \to o} \frac{\log N(\varepsilon)}{\log(\frac{1}{\varepsilon})} \tag{4.1}$$

exists, it will be called the dimension of the attractor. An important characteristic of a strange attractor is that D is small even though d is large. We should be interested in knowing whether transitional and turbulent signals have this property.

To see what the dimension means, let us write (4.1) as

$$N(\varepsilon) \sim \varepsilon^{-D}; \tag{4.2}$$

that is, if one specifies D and the accuracy $\varepsilon$ to which we need to determine the attractor, we automatically know the number of cubes required to cover the attractor. The only missing information will now be the position of the cubes in the phase space. Thus, D can be considered as a measure of how much more information is required in order to specify the attractor completely; the larger the value of D, the larger is this missing information.

In general, the dimension D, as defined in (4.1), is fractional for strange attractors, and it has been called the fractal dimension by Mandelbrot [30] who has contributed a lot to our understanding of the quantity. As defined in (4.1), D is a geometric property of the attractor, and does not take into account the fact that a typical trajectory may visit some region of the phase space more frequently than others. Several measures, taking this probability into account, have been defined — and are believed to be closely related to the dynamical properties of the attractor. The most well-known among them are:

(a) the pointwise dimension

(b) the Grassberger-Proccacia dimension.

If the attractor is uniform, that is, every region in the phase space is as likely to be visited by the trajectory as every other, then the above two measures equal D defined by (4.1). Otherwise, they are generally smaller than D.

Let $S_\varepsilon(x)$ be a sphere of radius $\varepsilon$ centered about a point x on the attractor, and let $\mu$ be the probability measure on the attractor. Then, the pointwise dimension is defined [31] as

$$d_p(x) = \lim_{\varepsilon \to o} \frac{\log \mu[S_\varepsilon(x)]}{\log \varepsilon} \tag{4.3}$$

or

$$\mu[S_\varepsilon(x)] \sim \varepsilon^{d_p} \tag{4.4}$$

Grassberger & Procaccia [32] have defined another measure $\nu$ which is related to the dimension of the attractor, as well as the entropy (see section 4d). The pro-

cedure for computing $\nu$ is as follows:

(i) Obtain the correlation sum $C(\varepsilon)$ from:

$$C(\varepsilon) = \lim_{N\to\infty} \frac{1}{N^2} \sum_{\substack{i=j=1 \\ i\neq j}}^{N} H[\varepsilon - |\underset{\sim}{u}_i - \underset{\sim}{u}_j|] \tag{4.5}$$

where H is the Heaviside step function and $\underset{\sim}{u}_i - \underset{\sim}{u}_j$ is difference in the two vector positions $\underset{\sim}{u}_i$ and $\underset{\sim}{u}_j$ on the phase space. Basically, what C does is to consider a window of size $\varepsilon$, and start a clock that ticks each time the difference $|\underset{\sim}{u}_i - \underset{\sim}{u}_j|$ lies within the box of size $\varepsilon$. Thus, one essentially has

$$C(\varepsilon) = \lim_{N\to\infty} \cdot \frac{1}{N^2} \{\text{number of pairs of points } (i,j) \text{ with } |\underset{\sim}{u}_i - \underset{\sim}{u}_j| < \varepsilon\}.$$

(ii) Obtain $\nu$ from the relation [32]

$$C(\varepsilon) \sim \varepsilon^{-\nu} \quad \text{as } \varepsilon\to o. \tag{4.6}$$

In practice, not all components of $\underset{\sim}{u}$ are known for constructing the phase space, but perhaps only one component, say $u_m$. As we discussed in section 3, one constructs a d-dimensional 'phase space' using delay coordinates

$$\{u_m(t_i),\ u_m(t_i+\tau),\ \ldots,\ u_m(t_i+(d-1)\tau)\},\ i = 1,\ \ldots, k,$$

where, again, $\tau$ is some interval which is neither too small nor too large and k is large (in principle, infinity!). Since one does not *a priori* know $\nu$, one constructs several 'phase spaces' of increasingly large value of d and evaluates $\nu$ for each of them; $\nu$ will first increase with d and eventually asymptote to a constant independent of d. This asymptotic value of $\nu$ is of interest to us as a measure of the dimension of the strange attractor.

We have computed both $d_p$ and $\nu$ as described above, using the streamwise velocity fluctuations u up to an Re of $10^4$, and the delay coordinates. Our confidence in the numerical values of these measures of dimension is very good when they are less than about 5 or 6, but becomes increasingly shaky at higher values. However, we do believe that they are reasonable, judging from their repeatability and the several precautions we have taken (such as taking the proper limit as $\varepsilon\to o$ and using, in a couple of cases, double precision arithmetic in our computations). It would be interesting and useful to evaluate the dimension at high Reynolds numbers, but such calculations are likely to be of uncertain value (unless perhaps some carefully selected combination of experimental and computational conditions obtains): with increasing Re, the newly excited degrees of freedom can be expected to be of smaller and smaller scales, and to properly accommodate them in the dimension calculations

requires that one must in practice look at increasingly smaller values of $\varepsilon$ (see equation 4.6). Such efforts will very soon be frustrated by instrumentation noise and digitizer resolution problems.

b. Data for Re $\lesssim$ 100

It is convenient to consider first the data for Re $\lesssim$ 100 (figure 17). Concentrating on the data in the ordered states only, we may conclude the following. At Re = 36, where there is only one independent degree of freedom (corresponding to the periodic vortex shedding) — see figures 2 and 5 — the dimension of the attractor turns out to be about 1. When only two frequencies are present (figures 3 and 6) at Re = 54, the dimension is about 2. At Re = 76 where there are three dominant frequencies (figure 10), the dimension is three to within experimental uncertainty. Lastly, at Re = 91 where there are four frequencies present, the calculated $\nu$ is very close to 4. Thus, to within computational uncertainties, it is seen that the dimension of the attractor is a reasonable representation of the number of degrees of freedom.

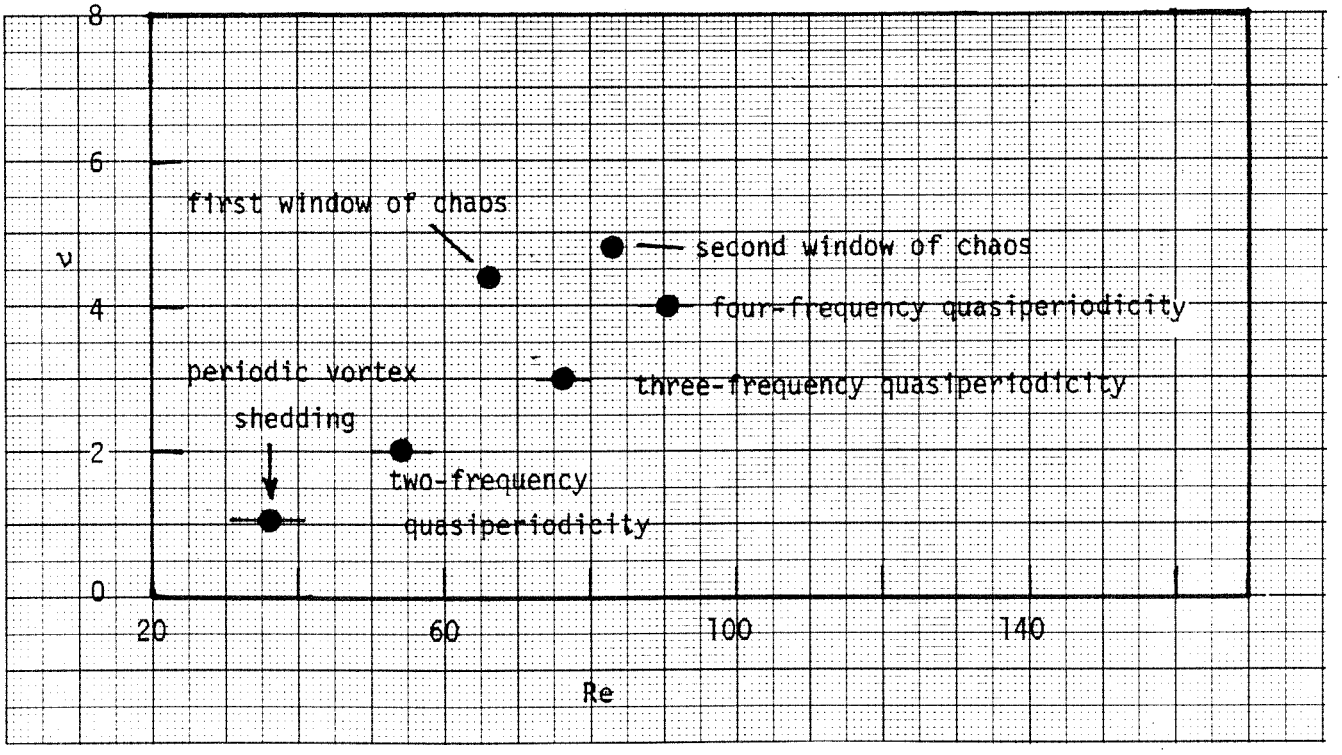


FIGURE 17: Variation of the dimension of the attractor with respect to Reynolds numbers. Note that the dimension is about 1 when there is only vortex shedding (Re = 36), about 2 when there are only 2 frequencies (Re = 54), about 3 when there are 3 frequencies (Re = 76), about 4 when there are 4 frequencies. The dimension jumps to higher noninteger values in the windows of chaos.

Now getting back to measurements in the windows of chaos, it is clear that the

first appearance of chaos at Re = 66 is characterized by a jump in the dimension (to about 4.4 from 2 characteristic of the two-frequency quasiperiodicity), followed by a return to a value of 3 in the region of three-frequency quasiperiodicity. Similarly, the dimension of the attractor in the second chaotic window is about 4.8. As we discussed earlier, the dimension of the attractor in the chaotic windows is a fraction.

c. Higher Reynolds number data

Figure 18 shows the results of the dimension calculations up to an Re of about $10^4$. Both $\nu$ and $d_p$ increase to about 20 or so at an Re of $10^4$, although the increase is not always monotonic. In fact, our calculations seem to suggest that the dimension settles down to about a value of 20!

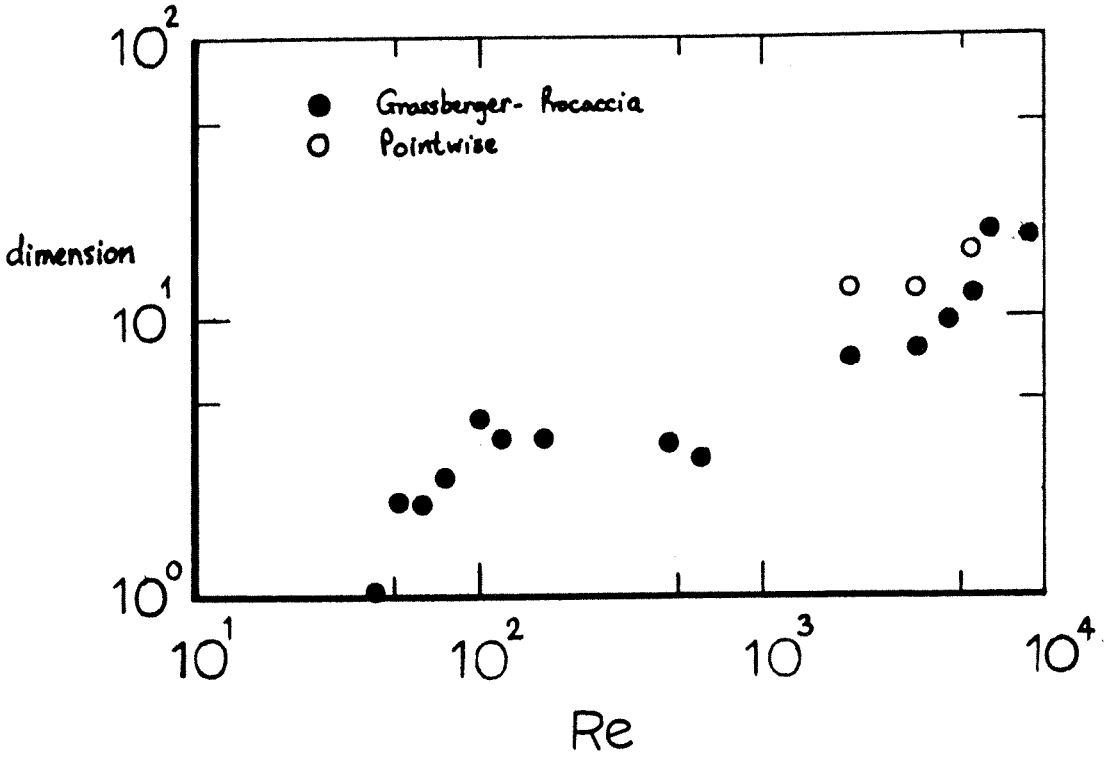


FIGURE 18: Dimension data for Re up to $10^4$.

If it is true that the dimension of the attractor retains, even at high Reynolds numbers, its meaning as an indicator of the number of dynamically significant degrees of freedom, common wisdom tells us that the dimension of the attractor should generally increase with Re. In contrast, the dimension does not increase continuously; further, its value is far lower than $Re^{9/4}$, which is the classical estimate (see Landau & Lifshitz [33]) for the number of degrees of freedom in a turbulent *flow*. It may be that the constancy of the dimension at higher Re is simply an artifact of re-

solution and computational problems, but if the result is genuine instead, it should provide an incentive for a suitable reformulation of 'turbulence problem'.

### d. The Kolmogorov entropy

The Kolmogorov entropy has the property that it is positive for a chaotic signal, zero for ordered signals and infinite for a random signal with a space filling attractor. As already mentioned, there are conjectures that the entropy equals the sum of positive Lyapunov exponents, and hence, unlike the dimension D, is a dynamic measure of unpredictability of the motion.

Suppose the d-dimensional phase space housing the attractor is partitioned into boxes of size $\varepsilon^d$. Let $p(i_1, i_2, \ldots, i_d)$ be the joint probability of finding $\underset{\sim}{u}$ at time $t = \tau$ in box $i_1$, $\underset{\sim}{u}$ at time $t = 2\tau$ in box $i_2$, ....., $\underset{\sim}{u}$ at time $t = d\tau$ in box $i_d$. The Kolmogorov entropy is then defined [34] as

$$K = - \lim_{\varepsilon \to o} \lim_{\tau \to o} \lim_{d \to \infty} \frac{1}{d\tau} \sum_{i_1, \ldots i_d} p(i_1, \ldots i_d) \ln p(i_1, \ldots i_d). \qquad (4.7)$$

Grassberger & Procaccia [35] have defined a quantity $K_2$ which is close to K and further has the property that $K_2 > 0$ is a sufficient condition for chaos. Without going into too many details, we follow [35] and note that it can be computed by first obtaining $C(\varepsilon)$ as in Eq.(4.5) in section 4a for various d, and forming the ratio

$$K_{2,d}(\varepsilon) = \frac{1}{\tau} \ln \frac{C_d(\varepsilon)}{C_{d+1}(\varepsilon)}, \qquad (4.8)$$

where $C_d$ indicates C for dimension d. In the limit,

$$\lim_{\substack{d \to \infty \\ \varepsilon \to o}} K_{2,d}(\varepsilon) \sim K_2.$$

Table 2 gives $K_2$ for Re = 66 and 81 within the first two windows of chaos. For comparison, the table also lists $K_2$ for the Hénon map from [35].

| Signal | $K_2$ |
|---|---|
| u at Re = 66 | $\approx 0.22$ |
| u at Re = 81 | $\approx 0.24$ |
| The Hénon map | $0.325 \pm 0.02$ |

Table 2: The Kolmogorov entropy

## 5 DISCUSSION OF RESULTS

We have shown that several features of transition to turbulence behind circular cylinders are in essential agreement with the behavior of low-dimensional dynamical systems. We emphasize that many details discussed above in the near-wake region hold also at around $x/d \simeq 50$, although less conspicuously.

One particularly important feature of this work is the discovery of windows of chaos interspersed between regions of order: these latter regions are three and four-frequency quasiperiodicities in the low Reynolds number range up to about 140 (possibly even higher!). Not all observations we have made can be understood within the present framework of chaos and dynamical systems, but we find it amazing that the dynamics of fluid motion which we believe are particularly governed by the NS equations should be at all represented by extremely simple systems. One aspect of this work is the fine resolution (in Reynolds number, frequency domain, as well as in the phase space) with which measurements have been made. It seems to us that even finer resolution, especially within the windows of chaos and regions bordering them, will perhaps disclose even more interesting aspects.

We have shown that, during early stages of transition, a strong connection (speculated previously, but never shown to be true conclusively) exists between the dimension of the attractor and the degrees of freedom as inferred from power spectral densities. Provided this interpretation is true also in windows of chaos and (moderately) high Reynolds number turbulence, our results suggest that the degrees of freedom are not too many even up to Reynolds number of the order of $10^4$. Our numerical calculations based on Schewe's data lead us to expect that the dimension of the attractor, as computed according to (4.4) and (4.5), is not high even at higher Reynolds numbers corresponding to the fully turbulent state ($Re \approx 10^6$). If the attractor is sufficiently low-dimensional, a clever projection of it can perhaps be used to our advantage. (If the attractor dimension is even as high as 20, however, no matter what projection one devises, it will perhaps look uniformly dark!) At this stage it is not clear how one could use this information, but, without entering into a detailed discussion, we may point out that it lends credence to concepts embodied in renormalization group theory, slaving principle, or, closer to home, large eddy simulation or orthogonal decomposition techniques.

We thus believe that there is much that we can learn about transition and turbulence from chaos theories. In the immediate future, these theories provide a strong motivation for looking into newer aspects of fluid flow phenomena; discoveries of close correspondence between fluid flows and low-dimensional chaotic dynamical systems will undoubtedly prove useful in the sense that the rich variety of results from dynamical systems can be brought to bear on fluid flow transition and, perhaps, even turbulence. In the long run, the hope is that they will help us in coming to grips with the eternal problem of turbulence, namely, the enormous amount of 'information'

that seems to be available to us! Perhaps we can then model, even at high Reynolds numbers, at least local behaviors by low-dimensional dynamical systems.

Do we then conclude that the key to the understanding of transition and turbulence lies totally in low-dimensional dynamical systems? We think that such statements are optimistic at best and misguided at the worst. Apart from the fact that the spatial structure of turbulent flows, which is their single most important characteristic, lies outside the scope of dynamical systems theories — at least as they stand today — there is a lot that they do not or, perhaps, cannot, tell: for example, they do not tell us anything about the origin and physical structure of the various bifurcations that can occur, or how the drag coefficient varies with Reynolds number. To answer these and similar questions of practical interest, we suspect that we have to revert to the NS equations!

One final comment should be made. It would be useful to make a concurrent flow visualization study and relate the various findings reported here to the spatial characteristics of the flow. It is unfortunate that we cannot use much the extensive flow visualization observations made by others (for example, Gerrard [36]) because the details from one experiment to another do not precisely match.

ACKNOWLEDGEMENTS

For their helpful comments during this work or on an earlier draft of the manuscript, it is my pleasant duty to thank Hassan Aref, Peter Bradshaw, B.-T. Chu, Rick Jensen, John Miles, Mark Morkovin, Turan Onat, David Ruelle, Paul Strykowski, Harry Swinney and Peter Wegener. I am indebted to Mike Francis who patiently accommodated this pursuit within an AFOSR grant I received for turbulence control work. Finally, presentation of these results in Evanston and preparation of this manuscript for this volume honoring Stan Corrsin has been a labor of love, and an expression of indebtedness I have for him.

APPENDIX

Let $b_1, b_2, \ldots, b_n$ be the state variables of the system (1.1). In an n-dimensional space spanned by $b_1, b_2, \ldots, b_n$, each point determines the state of the system completely at a given time, t. As t evolves, we obtain a continuous sequence of points which form the trajectory of the system. As $t \to \infty$, the $b_i$'s need not go to infinity, but may terminate (in two dimensions) either at a node or a focus or on a limit cycle or, in higher dimensions, on to a more complicated object. This object on which the trajectory terminates is called an attractor if all other trajectories starting near the said trajectory converge to the same object as $t \to \infty$. (That is, the

attractor is the limit set of a representative point in phase space. Thus, an attractor attracts all nearby trajectories.)

If the system is stable and steady the attractor is a point — a node if the motion is critically damped (figure A1) or a focus if the motion is damped but oscillatory (figure A2). If the system executes a periodic motion, a limit cycle is observed in the phase plane (figure A3). Quasiperiodic motion with two incommensurate frequencies results in a two-torus (see figure A4), with the entire surface of the torus covered by the trajectory eventually. A projection of the torus on to a plane may have different shapes depending on the orientation of the plane, but it is clear that a section of the torus, say, by the plane A in figure A4 (the Poincaré section) will yield a limit cycle. To obtain such a section in practice, one has to intercept the trajectory each time it crosses the plane (or 'sample' the system at the frequency $f_1$ and at fixed phase), and plot $b_1$ and $b_2$ (say) corresponding to these periodically sampled data. The phase portrait corresponding to the quasiperiodic motion with three frequencies is a three-torus, and so on.

The attractor has been called a 'strange attractor' if (roughly speaking) it is a complex surface repeatedly folded onto itself in such a manner that a line normal to the surface intersects it in a Cantor set. That is, if one successively magnifies regions of this intersection which appear, at some level of resolution, to be entirely 'filled', one sees regions of 'emptiness' interspersed between regions of 'occupation'. One cannot test this property of the strange attractor directly if it is constructed from experimental data (because of noise and the finite resolution of the instrumentation), and so, one uses several of its other properties to determine its occurrence. For example, any two neighboring trajectories on the strange attractor will diverge exponentially apart for small t (the so-called sensitivity to initial conditions, measured by positive Lyapunov exponents or the Kolmogorov entropy); the so-called dimension of the attractor (see section 4) is generally a non-integer; the spectral density of the temporal signal used to construct the attractor will have broadband components orders of magnitude above the instrumentation and other noise levels.

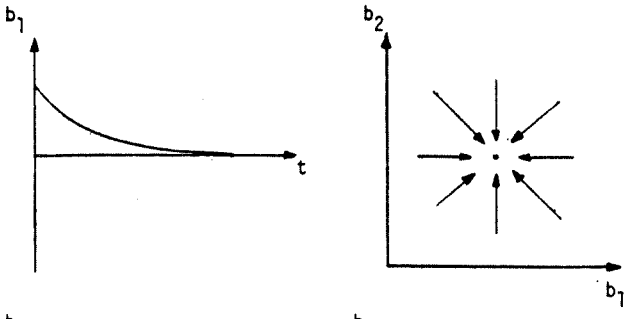


FIGURE A1: stable node.
(point attractor)

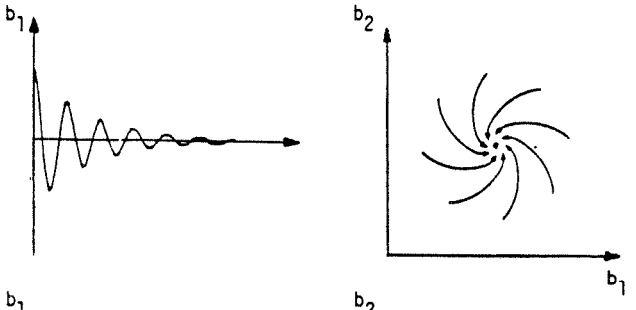


FIGURE A2: stable focus.
(point attractor)

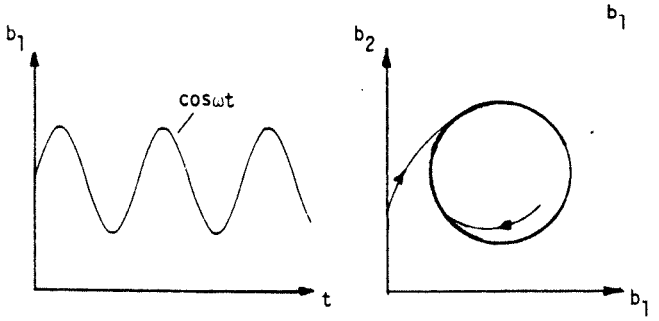


FIGURE A3: limit cycle.

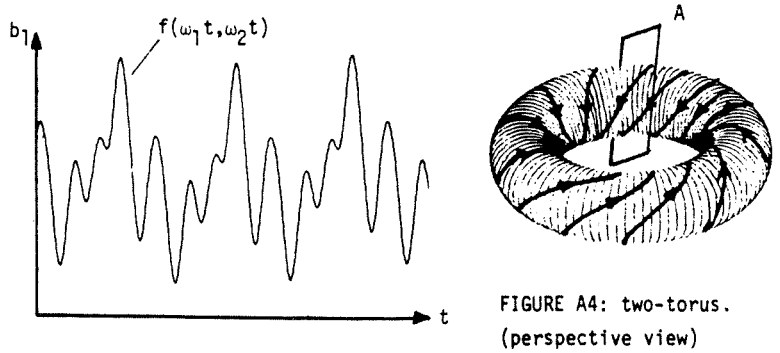


FIGURE A4: two-torus.
(perspective view)

REFERENCES


1. Ruelle, D. & Takens, F., Commun. Math. Phys. 20, 167 (1971).
2. Newhouse, S., Ruelle, D. & Takens, F., Commun. Math. Phys. 64, 35 (1978).
3. Gollub, J.P. & Swinney, H.L., Phys. Rev. Lett. 35, 927 (1975).
4. Fenstermacher, P.R., Swinney, H.L. & Gollub, J.P., J. Fluid Mech. 94, 103 (1979).
5. Brandstäter, A., Swift, J., Swinney, H.L. & Wolf, A., Phys. Rev. Lett. 51, 1442 (1983).
6. Libchaber, A. & Maurer, J., J. de Physique 41, C3-57 (1980).
7. Libchaber, A., In Chaos and Statistical Methods (ed. Y. Kuramoto, Springer 1984), p.221.
8. Coles, D., J. Fluid Mech. 21, 385 (1965).
9. Sreenivasan, K.R. & Strykowski, P.J., In Turbulence and Chaotic Phenomena in Fluids (ed. T. Tatsumi), to appear.
10. Sreenivasan, K.R., In Nonlinear Dynamics of Transcritical Flows (ed. H. Oertel), to appear.
11. Takens, F., In Lecture Notes in Mathematics 898 (eds. D.A. Rand and L.S. Young, Springer-Verlag 1981), p.366.
12. Chaitin, G.J., Scientific American, 246, 47 (May issue, 1982).
13. Thomas, R.M., J. Fluid Mech. 57, 549 (1973).
14. Gorman, M., Reith, L.A. & Swinney, H.L., Ann. N.Y. Acad. Sci. 357, 10 (1980).
15. Gollub, J.P., & Benson, S.V., J. Fluid Mech. 100, 449 (1980).
16. Greborgi, C., Ott, E. & Yorke, J.A., Phys. Rev. Lett. 51, 339 (1983).
17. Haken, H., Advanced Synergetics, Springer 1984.
18. Sparrow, C., The Lorenz Equations, Springer 1982.
19. Miles, J.W., Physica D (to appear), 1984.
20. Matsumoto, K. & Tsuda, I., J. Stat. Phys. 31, 87 (1983).
21. Roux, J.-C., Turner, J.C., McCormick, W.D., & Swinney, H.L., In Nonlinear Problems: Present and Future (eds. A.R. Bishop, D.K. Campbell, B. Nicolaenko, North-Holland Publishing Co., 1982), p.409.
22. Roshko, A., J. Fluid Mech. 10, 345 (1961).
23. Schewe, G., J. Fluid Mech. 133, 265 (1983).
24. Tritton, D.J., J. Fluid Mech. 6, 241 (1959).
25. Berger, E., Z. Flugwiss. 12, 41 (1964).
26. Tritton, D.J., J. Fluid Mech. 45, 749 (1971).
27. Friehe, C.A., J. Fluid Mech. 100, 237 (1980).
28. Gaster, M., J. Fluid Mech. 38, 565 (1969).
29. Malraison, B., Atten. P., Berge, P. & Dubois, M., J. Physique Lett. 44, L-897 (1983).
30. Mandelbrot, B., The Fractal Geometry of Nature, Freeman & Co., New York, 1983.
31. Farmer, J.D., Ott, E. & Yorke, J.A., Physica 7D, 153 (1983).

32. Grassberger, P. & Procaccia, I., Phys. Rev. Lett. 50, 346 (1983).
33. Landau, L.D. & Lifshitz, E.M., Fluid Mechanics (volume 6 of the Course of Theoretical Physics), Pergamon Press, 1982.
34. Barrow, J.D., Phys. Reports, 85, 1 (1982).
35. Grassberger, P. & Procaccia, I., Prepublication report (1983).
36. Gerrard, J.H., Phil. Trans. Roy. Soc. Lond. 288A, 29 (1978).